Supporting Information for:

Molecular dynamics study of naturally-occurring defects in self-assembled monolayer formation

*G. Gannon, J. C. Greer, J. A. Larsson and D. Thompson**

Tyndall National Institute, University College Cork, Ireland.

*To whom correspondence should be addressed: damien.thompson@tyndall.ie

Detailed explanation for the formation of the new "transition" region domain boundary

Figure A gives a time series of structure snapshots over 200 ps, showing the spontaneous formation of the transition region domain boundary in the right hand side of the simulation cell (see Figures 1-5 and 9 in the main text).

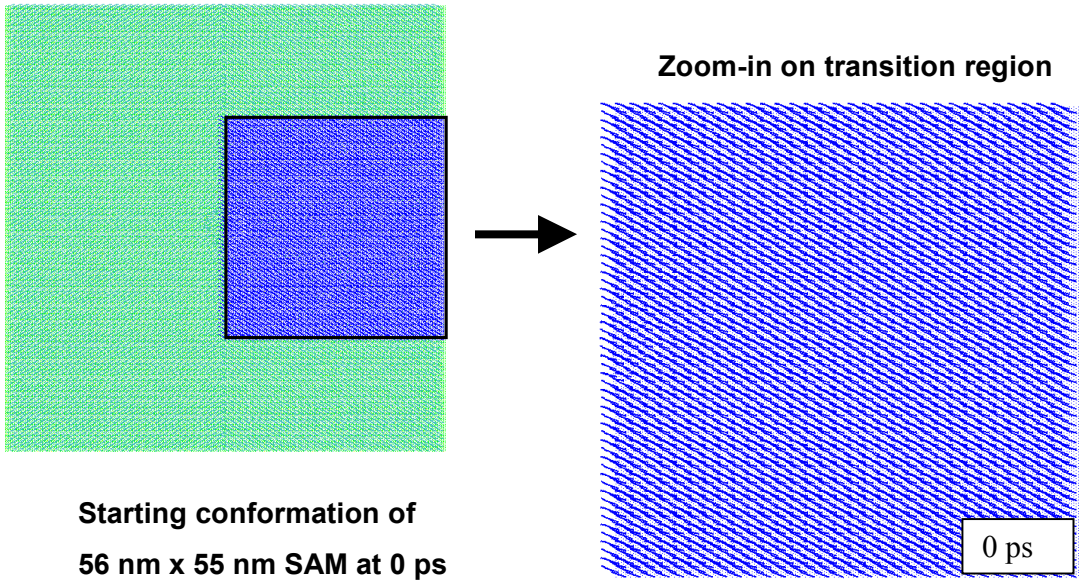

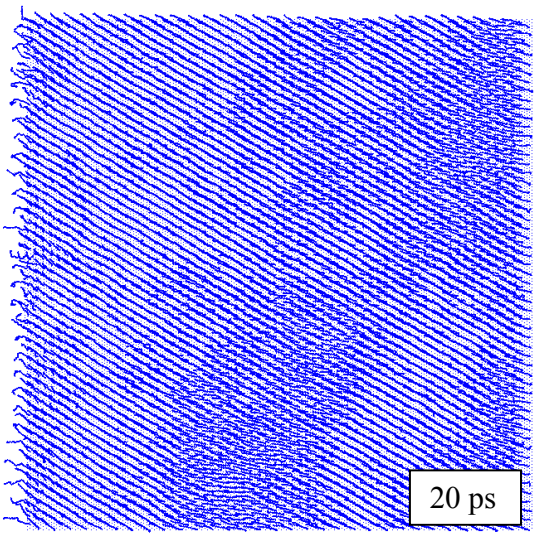
20 ps

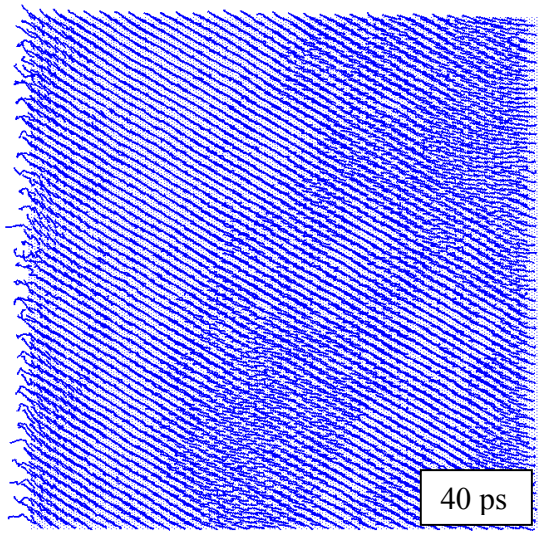
40 ps

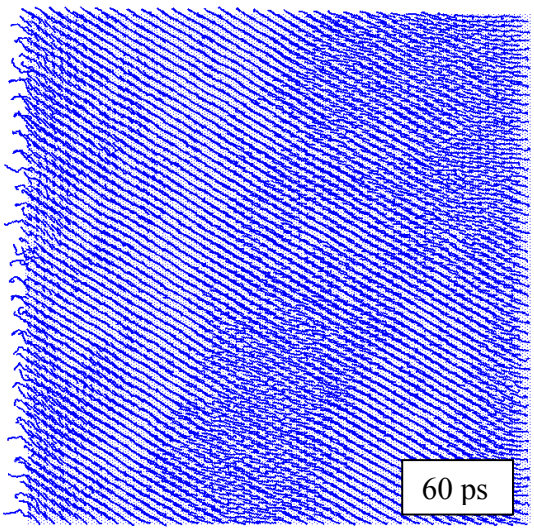
60 ps

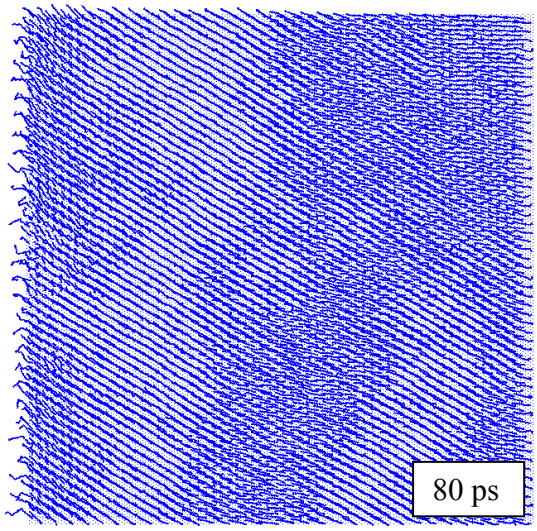
80 ps

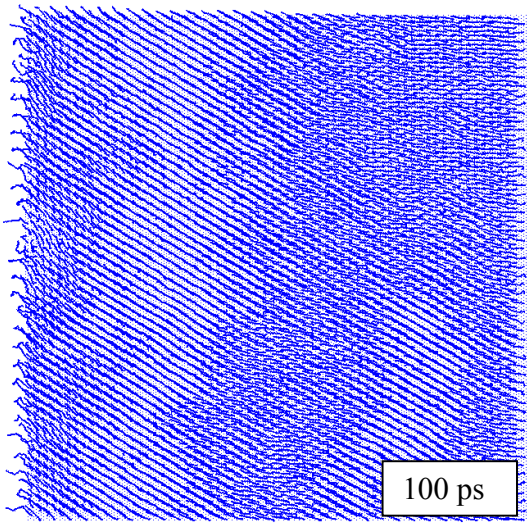
100 ps

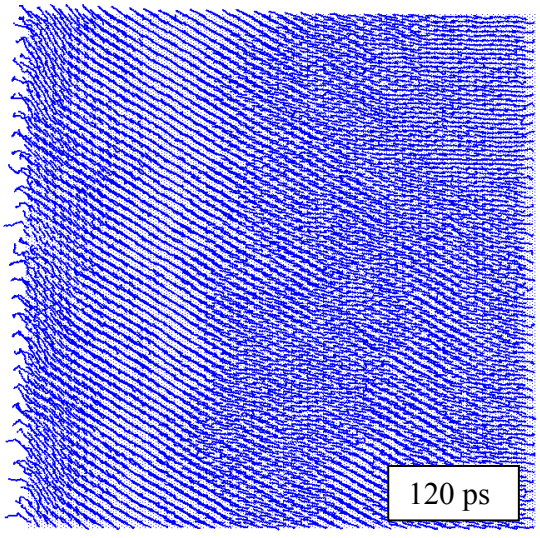
120 ps

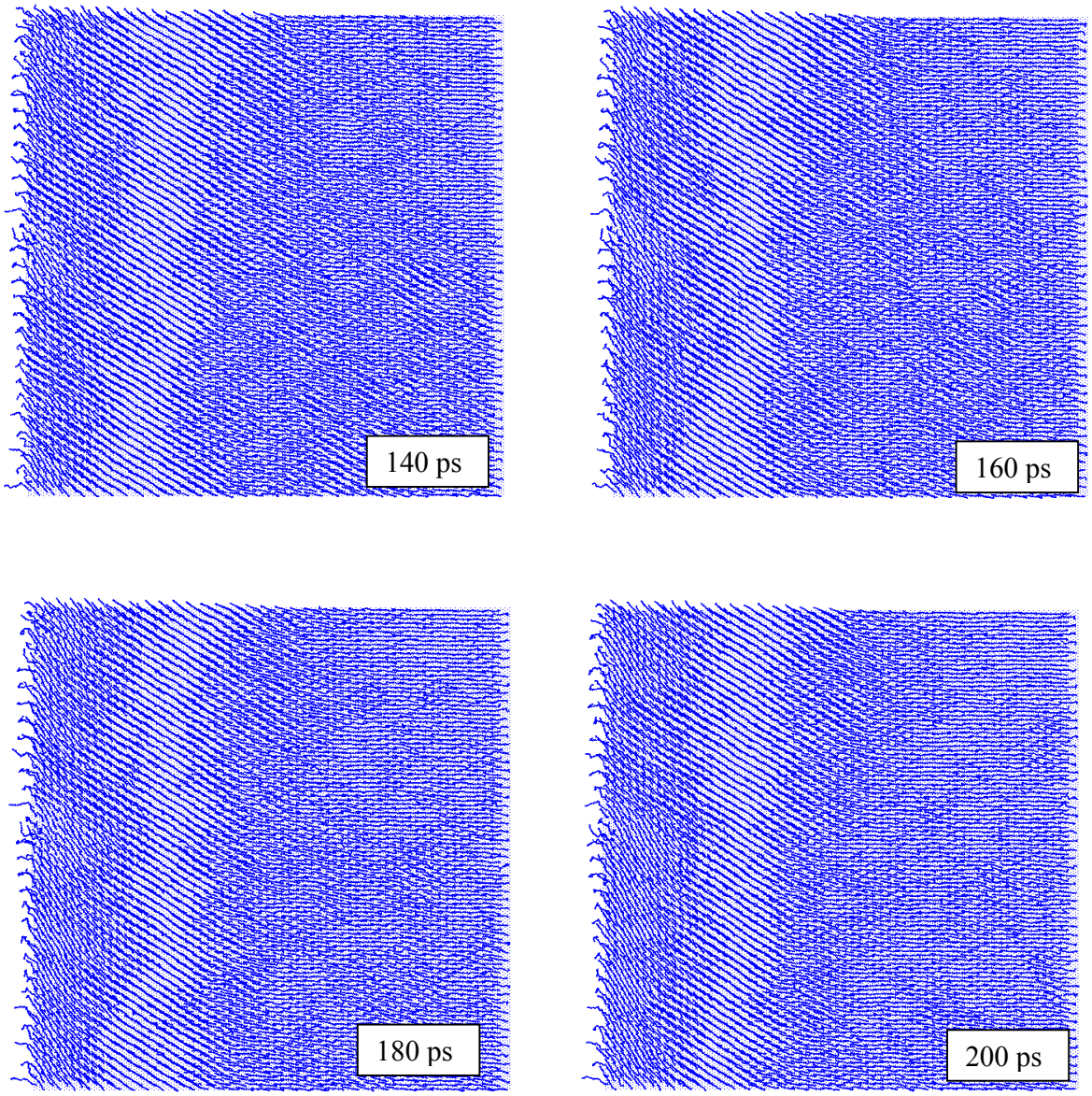

Figure A. Formation of the new “transition” region domain boundary.

A detailed explanation for the breaking of left/right symmetry in the simulation cell and formation of the new broad “transition” region domain boundary is given below.

In the starting simulation cell, the SAM chains on the left and right hand sides have precession angles of 156° and 19° respectively, as illustrated in Figure B below where the two domains are shown meeting at the "inwards" domain boundary.

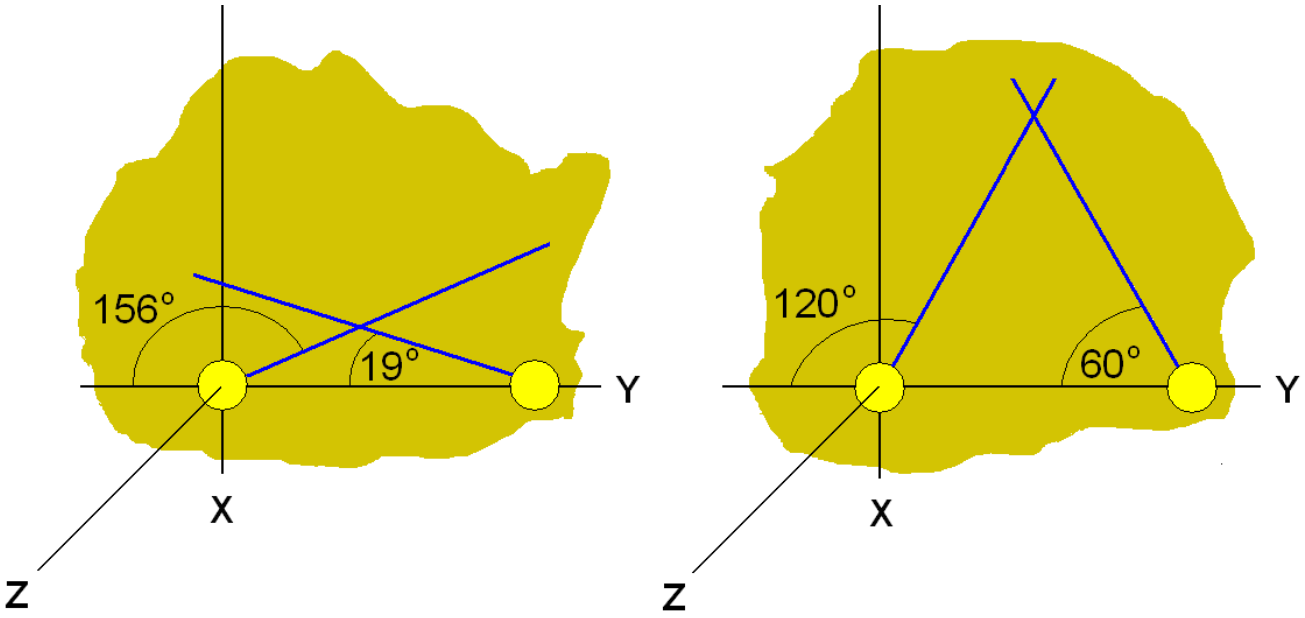

Figure B. The initial and relaxed precession angles of two opposing chains at the central "inwards" domain boundary are shown on the left and right hand side respectively, in plan view. The gold colored area represents the Au(111) surface in the xy plane, while the SAM chains are drawn in ball-and-stick format, with yellow spheres representing the terminal sulfur atoms and the blue lines representing the carbon backbone of the alkanethiol chains.

As shown in Figure C the system rearranges from this initial structure to find next-nearest neighbor, NNN, orientations within each domain, *i.e.* precession angles of a given integer multiple of 60° and so featuring the chains aligned with one of the three $\langle 10\bar{1} \rangle$ directions of the Au(111) surface, which lie 60° apart in space. SAM chains starting at 156° have two alternative precession angle values to rearrange to, 120° or 180°, while chains starting at 19° can rearrange to 0° or 60°. During the molecular dynamics simulations the chains relax so as to decrease the steric repulsion between opposing chains at the "inwards" domain boundary, by shifting to the left / right 120° / 60° precession angle arrangement illustrated above. The balance between intra- and inter-domain packing arrangements in the

periodic simulation cell means the interface does not relax further to, for example, a 60° / 60° precession angle arrangement at room temperature. Such relaxations may occur at room temperature at experimental timescales for some defect geometries but this does not occur within the 30 ns sampling time for our defect SAM model, occurring only at elevated temperatures (as shown in Figure 9 in the main text).

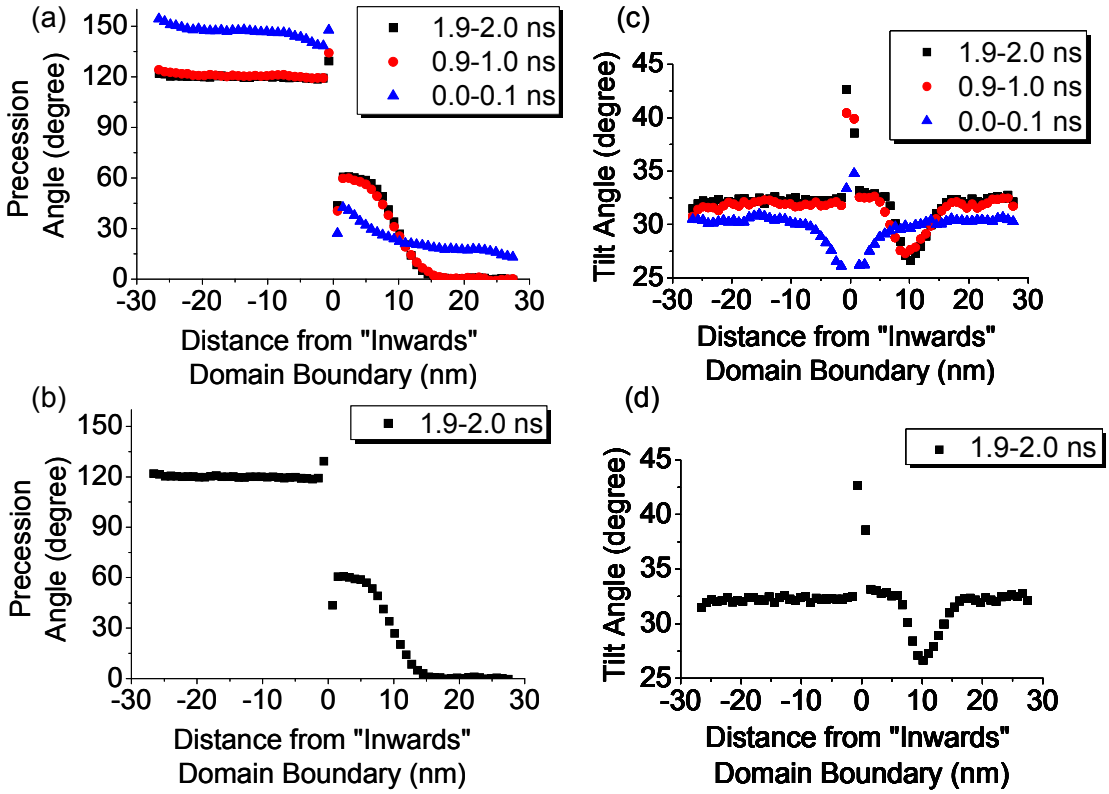

Figure C. "Pre-inked" SAM precession angle distribution, prior to the addition of the excess ink molecules, from the "inwards" domain boundary to the "outwards" domain boundary over (a) three different time segments, and (b) the final 1.9-2.0 ns of SAM relaxation. Pre-inked SAM tilt angle distribution, from the "inwards" domain boundary to the "outwards" domain boundary over (c) three different time segments, and (d) the final 1.9-2.0 ns of SAM relaxation.

The four accessible precession angle relaxations, to 180° and 120° on the left hand side and to 0° or 60° on the right hand side, provides a total of sixteen possible rearrangements, only four of which provide the sterically-required 120° / 60° relaxation at the "inwards" domain boundary. Describing each

of these four SAMs as a set of four possible precession angle domains, labeling from left to right across the simulation cell, gives the following four precession angle domain distributions: {120°, 120°, 60°, 0°}, {120°, 120°, 60°, 60°}, {180°, 120°, 60°, 0°}, and {180°, 120°, 60°, 60°}. The first is that found in the present simulations, as shown in Figure D (B) above, which features one "transition" region. The second features no transition regions, while the third and fourth feature respectively two and one "transition" regions. Assigning an equal weighting then to each of these four possible required rearrangements, we may estimate a probability of 75% for the formation of at least one "transition" region arising in the SAM. Many factors will influence the relative likelihood and lifetime of each possible domain distribution, including for example, the density of substrate and film defects, the distribution and shapes of different types of film domain boundaries, printing temperature and concentration of excess alkanethiol molecules.

In summary, the simulations show that when two domains meet and the domain boundary involves a steric clash, the interfacial chains will relax to give a difference in precession angles at the boundary equal to a multiple of 60°, which has the power to change the precession angle of a whole domain (for example, in our simulation cell, the left domain of the SAM in Figures 1-5 in the main text), but does not necessarily do so. If the change in precession angle is severe it is more favorable to create a ca. 5-10 nm wide domain boundary with a continuously changing precession angle, fulfilling a further 60° criterion to accommodate the original domain precession angle (for example, in our simulation cell, the right hand side of Figure 1 in the main text).